Available online at www.sciencedirect.com

SciVerse ScienceDirect

Ceramics International 38 (2012) 2667–2671

CERAMICS INTERNATIONAL

www.elsevier.com/locate/ceramint

Effect of pyrolysis temperature on the pore structure evolution of polysiloxane-derived ceramics

Liqun Duan, Qingsong Ma *

National Key Laboratory of Science and Technology on Advanced Ceramic Fibers &Composites, College of Aerospace & Materials Engineering, National University of Defense Technology, Changsha 410073, PR China

Received 28 July 2011; received in revised form 10 November 2011; accepted 12 November 2011
Available online 21 November 2011

Abstract

Homogeneous silicon oxycarbide (SiOC) ceramic powders were prepared by pyrolysis of cross-linked polysiloxane at different temperatures (1250–1500 °C) under vacuum. The effect of pyrolysis temperature on the pore structure evolution was investigated by means of N_2 adsorption, SEM, XRD, IR and element analysis (EA). Studies showed that predominate mesoporous ceramics with the average pore size in the range of 2–13 nm were obtained after pyrolysis in this temperature range. The pore structure transformation is strongly correlated with the thermolytic decomposition process of the used precursor, such as phase separation and carbothermal reduction. At relatively lower temperature (1250–1350 °C), the ceramics had a relative small specific surface areas (35 m^2/g) owing to the low degree of carbothermal reduction. However, as the carbothermal degree had an obvious augment at relative higher temperature (1400–1450 °C), the specific surface areas and total pore volume increased and reached to the maximum of 66 m^2/g and 0.214 cm^3/g, respectively, and subsequently decreased rapidly after 1500 °C for the reason of partial sintering of the nano-sized SiC derived from polysiloxane.

Keywords: Polysiloxane; Silicon oxycarbide; Pore structure; Pyrolysis temperature

1. Introduction

The conversion technology from preceramic polymers to Si-containing ceramics (SiOC, SiC, Si_3N_4, etc.) has attracted increasing attention in recent years for its advantages such as low processing temperature, controllable ceramic compositions through molecular design of precursor and near-net-shape technologies [1–6]. Of all the preceramic polymers, polysiloxane (PSO) has received increasing interest in recent years [7–9]. It is not only commercially available but also very cheap, and its derived silicon oxycarbide (SiOC) ceramics have been proved to possess improved properties such as microstructural stability and creep resistance over those of many conventional silicate ceramics [10,11].

The properties of polysiloxane derived ceramics depend on many factors, including material kind (proper compositions and molecule- network of polysiloxane), sample size, as well as pyrolysis system (final pyrolysis temperature, atmosphere, heating rate, etc.). Many articles have reported the pyrolysis behavior of polysiloxane under inert atmosphere, associating with its cross-linking, redistribution, mineralization, phase separation and crystallization [12–18]. However, the compositional and structural evolution of polysiloxane as a function of pyrolysis temperature under vacuum has not been explored very well, especially in the aspect of pore structure during its phase separation and carbothermal reduction process.

Hence, the aim of the present work is to study the effect of pyrolysis temperature on the pore structure evolution of polysiloxane-derived SiOC ceramics under vacuum.

2. Experiment

Commercially available polymethyl(phenyl)siloxane resin (Dow Corning 249 flake resin, density = 1.3 g/cm^3) is cross-linked at 250 °C in air for 4 h, and crushed into powders with a mean size of 180 μm. The experimental density of the cross-linked powders measured by densimeter method is 1.27 g/cm^3, which indicates nearly all pores are created due to pyrolysis.

* Corresponding author. Tel.: +86 731 84573169; fax: +86 731 84576578.
E-mail address: nudtmqs1975@163.com (Q. Ma).

0272-8842/$36.00
doi:10.1016/j.ceramint.2011.11.033

And then the powders were placed in graphite crucibles and pyrolyzed at different temperatures (1250–1500 °C) for 1 h under vacuum with a heating rate of 15 °C/min.

The N_2 adsorption–desorption isotherms were obtained using Quantachrome instruments at 77 K. BET analyses were used to determine the total specific surface area (S_{BET}). Non Local Density Functional Theory (NLDFT) method was used to analyze the pore size distributions (PSDs) and different pore volumes. SEM (JSM-5600LV, JEOL) observations were conducted to examine the microstructures. X-ray diffraction (Bruker D8 advance) with Cu Kα radiation was used to verify the crystal phases. IR spectra between 4000 and 400 cm^{-1} were carried out with a resolution of 4 cm^{-1} on a Thermo Niocolet Fourier Transform Spectrum, using the KBr disk method. Quantitative elemental analysis (EA) of the samples was performed on LECOCS600 for C. The perchloric acid dehydration gravimetric method was adopted for the determination of Si content. And the residue element is considered to be O. The densities of powders after pyrolysis at different temperatures were obtained using densimeter method.

3. Results and discussion

Fig. 1 shows the N_2 adsorption–desorption isotherms and the corresponding pore size distributions of the products. It turns out that all the samples show intermediate state of type II and type IV isotherms with H1 hysteresis according to IUPAC classification [19], implying that predominant mesopores

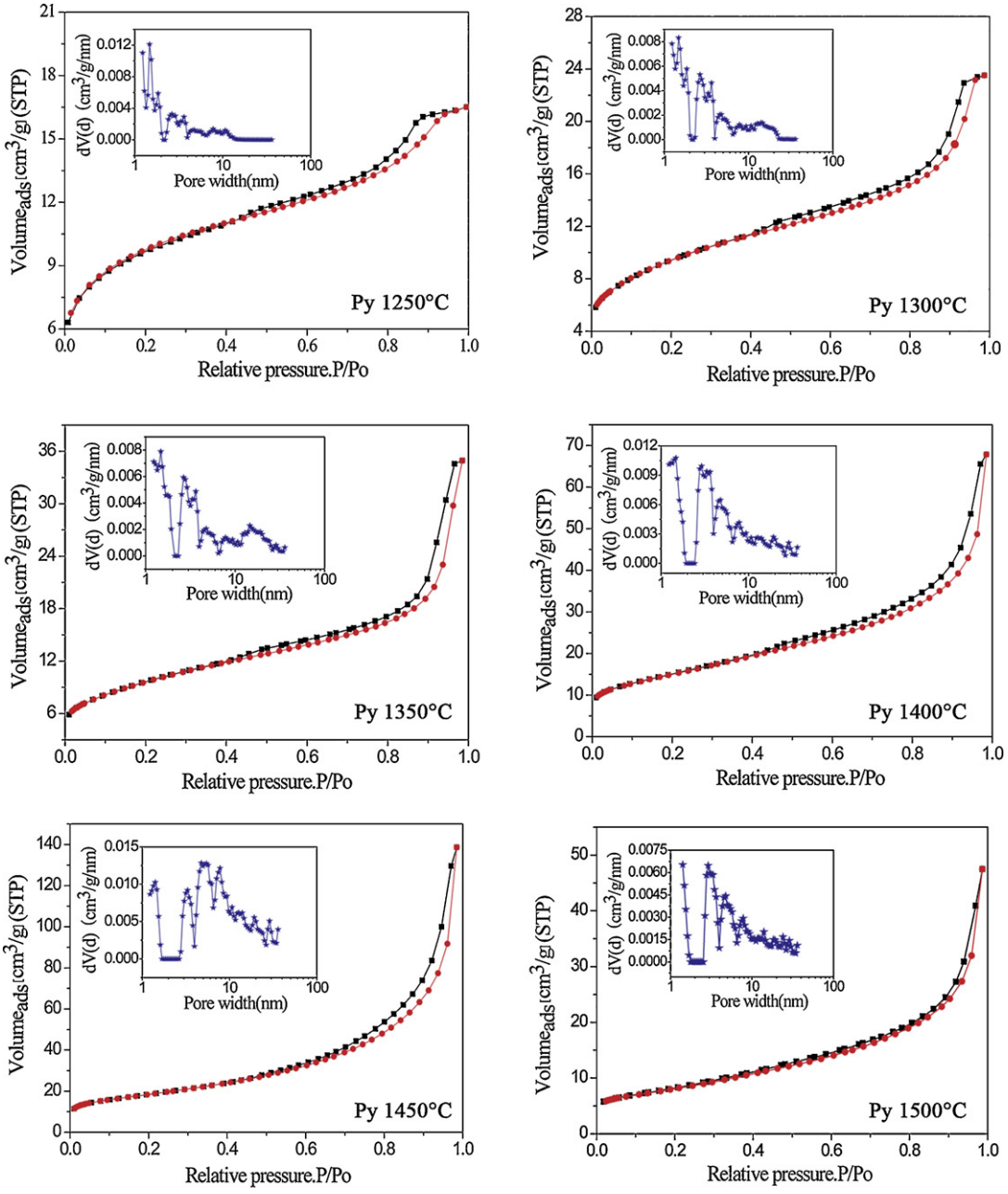

Fig. 1. Isotherm sorption and PSD curves of the products pyrolyzed at different temperatures.

Table 1
Pore parameters of the products pyrolyzed at different temperatures.

Temperature (°C)	BET surface area (m^2/g)	Average pore size (nm)	V^a (cm^3/g)	V^b (cm^3/g)	V^c (cm^3/g)	V^t (cm^3/g)
1250	35	2.9	0.011	0.013	0.002	0.026
1300	34	4.2	0.009	0.025	0.002	0.036
1350	35	6.2	0.008	0.042	0.004	0.054
1400	54	7.8	0.010	0.080	0.015	0.105
1450	66	13.1	0.009	0.170	0.035	0.214
1500	29	10.2	0.005	0.052	0.017	0.074

[a] Micropore; [b] mesorpore; [c] macropore; [t] total pore.
The macropore volume is calculated by the following equation: $V^c = V^t - V^a - V^b$.

($2 < d < 50$ nm) be generated during pyrolysis. The tiny initial vertical parts of the curve at low relative pressure reveal the presence of micropores ($d < 2$ nm). Further more, it can be shown that the vertical parts get smooth gradually at elevated temperatures, indicating the decreasing proportions of micropores. At high relative pressure ($P/P_0 > 0.9$), the isotherms have sharp increase, indicating that a quantity of macropores ($d > 50$ nm) exist in these pyrolyzed samples. The corresponding PSDs of all the samples pyrolyzed at different temperatures are also displayed within Fig. 1. We can see that pores generated by pyrolysis at different temperatures are multimodal and wide range distributed.

The different pore volumes and BET surface areas of the samples are summarized in Table 1. As the increasing of pyrolysis temperature, the proportion of micropores basically decreases from 42% to 4%. In contrast, the macropore volume increases from 7% to 23%. The mesopore volume changes with the same trend of total pore volume and its proportion is more than 50%. Besides, the average pore size for all the samples is in the mesopore range of 2–13 nm, implying that mainly mesoporous materials are obtained after pyrolysis.

Few changes for the BET surface areas can be observed below 1400 °C, except for small increase of pore volume. At higher temperature, the specific surface area and total pore volume increases with increasing pyrolysis temperature, and approaches a maximum of 66 m^2/g and 0.214 cm^3/g, respectively, when the pyrolysis temperature reaches 1450 °C. However, when the pyrolysis temperature was increased to 1500 °C, the elimination of nanopores ($0 < d < 100$ nm) with a high speed was observed, characterized by the decrease of specific surface area and total pore volume.

This result is well consistent with the results characterized by SEM method (Fig. 2). Changes are small at elevated temperature starting from 1250 °C up to 1350 °C. Above this temperature, a great distinguish was observed. More pores emerged between small ''particles'' with a diameter below 100 nm up to 1450 °C. Subsequently, most of the resulting pore disappeared, which led to the representation of sintering morphology for the sample pyrolyzed at 1500 °C.

These phenomena belonged to the pore structure evolution are strongly correlated with the thermolytic decomposition of the adopted precursor, especially in the process of phase separation and carbothermal reduction. The structural evolution from silicon resin to ceramic material, as a function of the pyrolysis temperature, was monitored by IR spectra (Fig. 3) and XRD method (Fig. 4). For the sake of clarity and perspicuity, the temperature range here is separated into two parts.

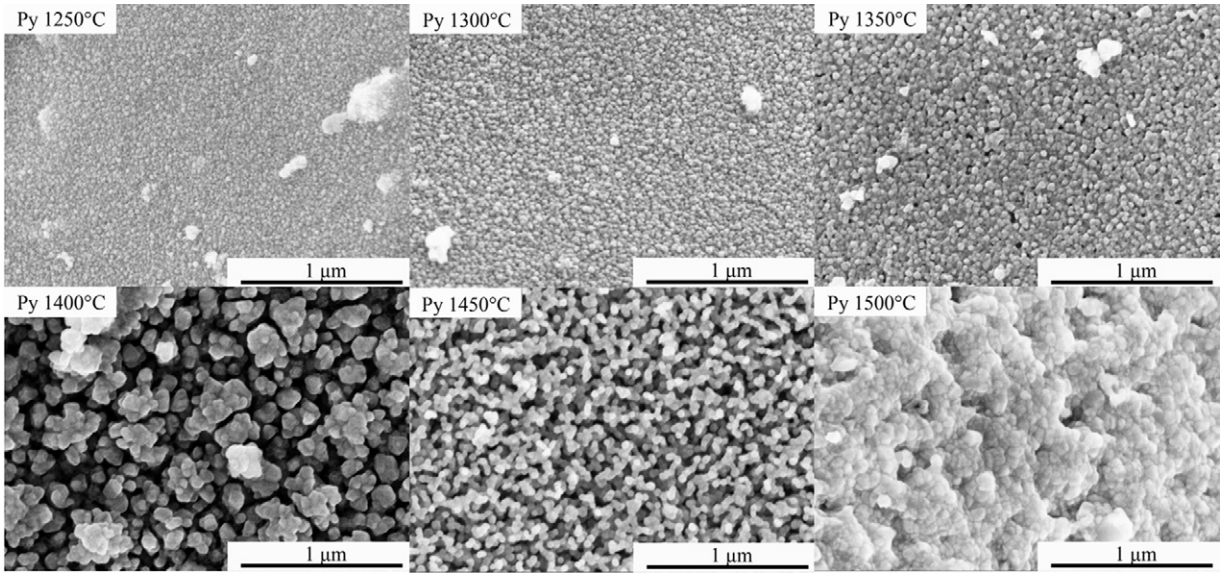

Fig. 2. SEM images of the products pyrolyzed at different temperatures.

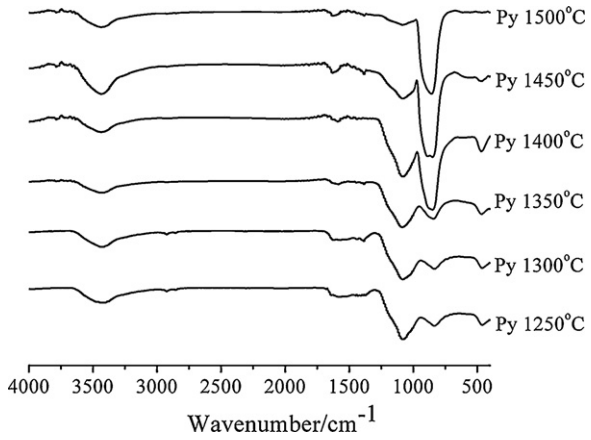

Fig. 3. IR patterns of the products pyrolyzed at different temperatures.

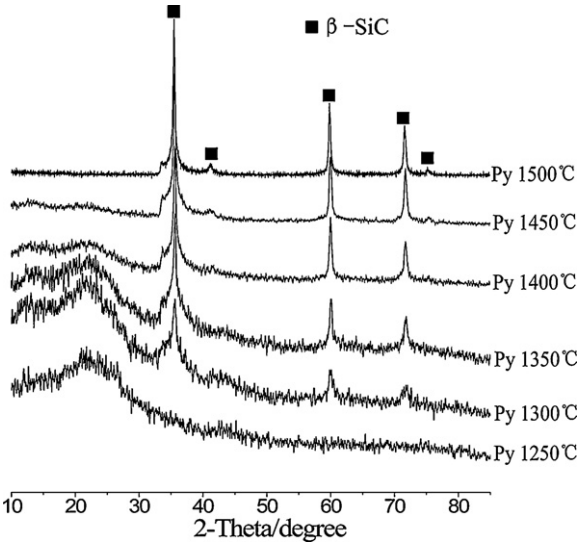

Fig. 4. XRD patterns of the products pyrolyzed at different temperatures.

(i) 1250–1350 °C: as shown in Fig. 3, two broad bands at 1081 and 842 cm^{-1} assigned mainly to νSi–O–Si and νSi–C absorptions, respectively, did not present a significant change in intensity. However, distinct transformation could be observed by XRD patterns, shown in Fig. 4. The resulting ceramics were completely amorphous when pyrolyzed at 1250 °C. When the final temperature increased to 1300 °C and 1350 °C, β-SiC phase could be detected, characterized by broad diffraction peaks at 35.6°, 41.4°, 60°, 71.8° and 75.5° (2θ), corresponding to (1 1 1), (2 0 0), (2 2 0), (3 1 1) and (2 2 2) SiC phases, respectively [20]. The samples also showed a broad halo centered at ∼22°, typical of amorphous silica phase [21]. It can be inferred that carbothermal reduction is not dominated in this temperature range, and SiC nanocrystallines were mainly yielded by phase separations process: $SiC_xO_{2(1-x)} \Rightarrow xSiC + (1-x)SiO_2$, which was observed by Xu et al. [22]. SiC phase and amorphous silica phase other than gaseous molecules were generated, which contributed little to the pore-forming process. That is why powdered samples with relative small and stable BET surface areas were obtained in this temperature range.

(ii) 1400–1500 °C: a distinct enhancement of the relative intensity of the absorption centered at 842 cm^{-1} (νSi–C) was verified when the pyrolysis temperature changed from 1350 °C to 1400 °C (Fig. 3). The relative intensity of the absorption (νSi–O) decreased at elevated temperature, contrary with that of SiC diffraction peaks (Fig. 4). The broad halo became smaller and smaller, and can hardly be observed for the sample pyrolyzed at 1500 °C. Table 2 shows the density and elemental composition of the products pyrolyzed at different temperatures. We can see the value of density increases with a high speed after 1400 °C and gets close to that of pure silicon carbide (3.2 g/cm^3). Chemical composition of the samples shows clearly the quick reduction of free carbon content, especially for the samples pyrolyzed at 1400–1500 °C. It can be concluded that carbothermal reduction is dominate in this temperature range, $SiO_2 + 3C \Rightarrow SiC + 2CO_{(g)}$. Consequently, much small gaseous molecules (CO) released from the samples and generated pores simultaneously, leading to the augment of BET surface areas and total pore volume of the pyroylzed samples. Based on the pyrolyzed composition at 1500 °C (Table 2), the sample still contains excess carbon (∼4.7 wt.%). The composition containing Si–O–C is most likely ''SiC + SiO_2 + excess carbon''. A weak absorption at 1081 cm^{-1}, characteristic of νSi–O can still be detected for the sample pyrolyzed at 1500 °C (shown in Fig. 3), indicating a residue of silica. Nevertheless, the carbothermal reduction of SiO_2 by excess carbon may compete with partial sintering of

Table 2
Density and elemental composition of the products pyrolyzed at different temperatures.

Temperature (°C)	Density (g/cm^3)	Composition (wt.%)			Atomic formula	Calculated composition	Free carbon (wt.%)
		Si	O	C			
1250	1.96	35.43	27.92	36.65	$SiO_{1.38}C_{2.41}$	$SiO_{1.38}C_{0.31} + 2.10C_f$	31.9
1300	1.99	40.23	23.25	36.52	$SiO_{1.01}C_{2.12}$	$SiO_{1.01}C_{0.49} + 1.63C_f$	28.1
1350	2.04	42.32	21.51	36.17	$SiO_{0.89}C_{1.99}$	$SiO_{0.89}C_{0.55} + 1.44C_f$	26.1
1400	2.22	45.70	18.96	35.34	$SiO_{0.73}C_{1.80}$	$SiO_{0.73}C_{0.64} + 1.16C_f$	22.7
1450	2.47	56.96	9.26	33.78	$SiO_{0.28}C_{1.38}$	$SiO_{0.28}C_{0.86} + 0.52C_f$	12.7
1500	2.83	65.51	2.99	31.50	$SiO_{0.08}C_{1.12}$	$SiO_{0.08}C_{0.96} + 0.16C_f$	4.7

Atomic formula is based on the formula SiO_xC_y [23].
Calculated composition is based on the formula $SiO_xC_{(1-x/2)} + y - (1-x/2)C_f$ [23].

polysiloxane-derived SiC at the near end stage of carbothermal reduction, because the polysiloxane-derived SiC is nano-sized [24] and can be sintered partially at 1500 °C due to its large surface energy [25]. Thus, partial sintering of the polysiloxane-derived SiC decreased the total pore volume and the specific surface area rapidly.

4. Conclusion

In summary, this study shows the effect of the pyrolysis temperature on the pore structure evolution of the pyrolysates from silicon resin under vacuum. The pore structure evolution is mainly decided by the carbothermal reduction progress. Three stages are demonstrated corresponding to three consecutive stages of carbothermal progress, respectively. The first stage (1250–1350 °C): the ceramics had a relative small specific surface areas in the initial stage of carbothermal reduction progress; The second stage (1400–1450 °C): as the carbothermal progress proceeded to a relatively high point, the specific surface areas and total pore volume increased accordingly; The third stage (above 1450 °C): the specific surface areas and total pore volume decreased rapidly for the reason of partial sintering of polysiloxane-derived SiC at the near end stage of carbothermal reduction.

Acknowledgments

This study was supported by the Hunan Provincial Natural Science Foundation of China (no. S2010J504B) and National Defense Preliminary Research Program of China (no. 9140C8203040904).

References

[1] P. Colombo, G. Mera, R. Riedel, G.D. Sorarù, Polymer-derived ceramics: 40 years of research and innovation in advanced ceramics, J. Am. Ceram. Soc. 93 (2010) 1805–1837.
[2] Y. Tang, J. Wang, X.D. Li, W.H. Li, H. Wang, X.Z. Wang, Thermal stability of polymer derived SiBNC ceramics, Ceram. Int. 35 (2009) 2871–2876.
[3] Y. Iwamoto, K. Sato, T. Kato, T. Inada, Y. Kubo, A hydrogen-permselective amorphous silica membrane derived from polysilazane, J. Eur. Ceram Soc. 25 (2005) 257–264.
[4] G.Y. Li, X.D. Li, H. Wang, X. Xing, Y. Yang, SiC nanowires grown on activated carbon in a polymer pyrolysis route, Mater. Sci. Eng. B 166 (2010) 108–112.
[5] V. Liebau, R. Hauser, R. Riedel, Amorphous SiBCO ceramics derived from novel polymeric precursors, C.R. Chim. 7 (2004) 463–469.
[6] Z. Xie, S. Cao, J. Wang, X. Yan, S. Bernard, P. Miele, Engineering of silicon-based ceramic fibers: novel SiTaC(O) ceramic fibers prepared from polytantalosilane, Mater. Sci. Eng. A 527 (2010) 7086–7091.
[7] L. Biasetto, A. Francis, P. Palade, G. Principi, P. Colombo, Polymer-derived microcellular SiOC foams with magnetic functionality, J. Mater. Sci. 43 (2008) 4119–4126.
[8] C. Moysan, R. Riedel, R. Harshe, T. Rouxel, F. Augereau, Mechanical characterization of a polysiloxane-derived SiOC glass, J. Eur. Ceram Soc. 27 (2007) 397–403.
[9] Q.S. Ma, Y. Ma, Z.H. Chen, Fabrication and characterization of nanoporous SiO_2 ceramics via pyrolysis of silicone resin filled with nanometer SiO_2 powders, Ceram. Int. 36 (2010) 2269–2272.
[10] G.M. Renlund, S. Prochazka, R.H. Doremus, Silicon oxycarbide glasses: Part II. Structure and properties, J. Mater. Res. 6 (1991) 2723–2734.
[11] L. Tian, Y.L. Li, D. Su, H.B. Du, Silicon oxycarbide ceramics with reduced carbon by pyrolysis of polysiloxanes in water vapor, J. Eur. Ceram Soc. 30 (2010) 2677–2682.
[12] M.R. Mucalo, N.B. Milestone, I.W.M. Brown, NMR and X-ray diffraction studies of amorphous and crystallized pyrolysis residues from pre-ceramics polymers, J. Mater. Sci. 32 (1997) 2433–2444.
[13] S. Martínez-Crespiera, E. Ionescu, H.J. Kleebe, R. Riedel, Pressureless synthesis of fully dense and crack-free SiOC bulk ceramics via photocrosslinking and pyrolysis of a polysiloxane, J. Eur. Ceram Soc. 31 (2011) 913–919.
[14] V. Belot, R.J.P. Corriu, D. Leclercq, P.H. Mutin, A. Vioux, Thermal redistribution reactions in crosslinked polysiloxanes, J. Polym. Sci. A Polym. Chem. 30 (1992) 613–623.
[15] A.M. Wilson, G. Zank, K. Eguchi, W. Xing, B. Yates, J.R. Dahn, Polysiloxane pyrolysis, Chem. Mater. 9 (1997) 1601–1606.
[16] J.H. Eom, Y.W. Kim, I.H. Song, H.D. Kim, Microstructure and properties of porous silicon carbide ceramics fabricated by carbothermal reduction and subsequently sintering process, Mater. Sci. Eng. A 464 (2007) 129–134.
[17] G.A. Danko, R. Silberglitt, Comparison of microwave hybrid and conventional heating of preceramic polymers to form silicon carbide and silicon oxycarbide ceramics, J. Am. Ceram. Soc. 83 (2000) 1617–1625.
[18] R. Harshe, C. Balanb, R. Riedel, Amorphous Si(Al)OC ceramic from polysiloxanes: bulk ceramic processing, crystallization behavior and applications, J. Eur. Ceram Soc. 24 (2004) 3471–3482.
[19] K.S.W. Sing, D.H. Everett, R.A.W. Haul, L. Moscou, R.A. Pierotti, J. Rouquerol, T. Siemieniewska, Reporting physisorption data for gas/solid systems, in: Handbook of Heterogeneous Catalysis, 2008, pp. 1217–1230.
[20] Z.X. Yang, W.M. Zhou, F. Zhu, Y.F. Zhang, SiC/SiO_2 core-shell nanocables formed on the carbon fiber felt, Mater. Chem. Phys. 96 (2006) 439–441.
[21] M.A. Schiavon, E. Radovanovic, I.V.P. Yoshida, Microstructural characterization of monolithic ceramic matrix composites from polysiloxane and SiC powder, Powder Technol. 123 (2002) 232–241.
[22] T.H. Xu, Q.S. Ma, Z.H. Chen, The effect of environment pressure on high temperature stability of silicon oxycarbide glasses derived from polysiloxane, Mater. Lett. 65 (2011) 1538–1541.
[23] V. Belot, R.J.P. Corriu, D. Leclercq, P.H. Mutin, A. Vioux, Silicon oxycarbide glasses with low O/Si ratio from organosilicon precursors, J. Non-Cryst. Solids 176 (1994) 33–44.
[24] K.J. Kim, S. Lee, J.H. Lee, M.H. Roh, K.Y. Lim, Y.W. Kim, Structural and optical characteristics of crystalline silicon carbide nanoparticles synthesized by carbothermal reduction, J. Am. Ceram. Soc. 92 (2009) 424–428.
[25] M. Fukushima, Y. Zhou, Y.I. Yoshizawa, Fabrication and microstructural characterization of porous silicon carbide with nano-sized powders, Mater. Sci. Eng. B 148 (2008) 211–214.